Laboratory Investigation (2019) 99:499–513
https://doi.org/10.1038/s41374-018-0135-3

ARTICLE

The role of Ca^{2+} in acid-sensing ion channel 1a-mediated chondrocyte pyroptosis in rat adjuvant arthritis

Xiaoshan Wu[1] · Guiling Ren[2] · Renpeng Zhou[3] · Jinfang Ge[3] · Fei-Hu Chen[3]

Received: 4 April 2018 / Revised: 22 June 2018 / Accepted: 18 July 2018 / Published online: 28 November 2018

Abstract

Rheumatoid arthritis is an autoimmune disease with a poor prognosis. Pyroptosis is a type of proinflammatory programmed cell death that is characterised by the activation of caspase-1 and secretion of the proinflammatory cytokines interleukin (IL)-1β/18. Previous reports have shown that pyroptosis is closely related to the development of some autoimmune diseases, such as rheumatoid arthritis. The decrease in the pH of joint fluid is a main pathogenic feature of RA and leads to excessive apoptosis in chondrocytes. Acid-sensitive ion channels (ASICs) are extracellular H^+-activated cation channels that mainly influence Na^+ and Ca^{2+} permeability. In this study, we investigated the role of Ca^{2+} in acid-sensing ion channel 1a-mediated chondrocyte pyroptosis in an adjuvant arthritis rat model. The expression of apoptosis-associated speck-like protein, NLRP3, caspase-1, ASIC 1a, IL-1β and IL-18 was upregulated in the joints of rats compared with that in normal rats, but the expression of Col2a in cartilage was decreased. However, these changes were reversed by amiloride, which is an inhibitor of ASIC1a. Extracellular acidosis significantly increased the expression of ASIC1a, IL-1β, IL-18, ASC, NLRP3 and caspase-1 and promoted the release of lactate dehydrogenase. Interestingly, Psalmotoxin-1 (Pctx-1) and BAPTA-AM inhibited these effects. These results indicate that ASIC1a mediates pyroptosis in chondrocytes from AA rats. The underlying mechanism may be associated with the ability of ASIC1a to promote $[Ca^{2+}]_i$ and upregulate the expression of the NLRP3 inflammasome.

Introduction

Rheumatoid arthritis (RA) is a chronic systemic autoimmune disease with a high incidence and a poor prognosis that mainly affects the ambient joints [1, 2]. The main pathological features of RA in patients, include hyperplasia of synovial cells, pannus formation and infiltration of a variety of inflammatory cells [3], causing erosion and destruction in articular cartilage and bone [4]. Studies have shown that the intra-articular accumulation of inflammatory metabolites results in a decrease in the pH of joint fluid, which can be reduced to a pH of 6.0 or even lower. The decrease in pH is a main pathogenic feature of RA that leads to excessive apoptosis in chondrocytes [5, 6], which eventually causes pathological changes in the joints. Studies have also found that the proinflammatory cytokines interleukin (IL)-1β, IL-6 and IL-18 play a vital role in the destruction of articular cartilage and chondrocyte apoptosis in RA [7]. Although many studies have recently investigated RA, the specific mechanism of RA remains vague. To date, the clinical treatment of RA includes anti-COX2 drugs, corticosteroid drugs, disease-modifying anti-rheumatic drugs and some novel biological drugs [8–12]. However, the limited efficacy and side effects of these drugs limit their clinical application; therefore, this disease still has a high rate of morbidity due to adverse cardiovascular complications and diabetes [13].

Pyroptosis is a type of proinflammatory programmed cell death [14] that is characterised by the activation of caspase-1 and the secretion of the proinflammatory cytokines IL-1β/18 [15–17]. Pyroptosis is closely related to the innate immune system, which is essential for resistance to infection by

✉ Fei-Hu Chen
cfhchina@sohu.com

1 The First Affiliated Hospital of USTC, Division of Life Science and Medicine, University of Science and Technology of China, Hefei, Anhui 230001, P.R. China

2 Department of Pharmacy, The 901 Hospital of Chinese People's Liberation Army Joint Service Support Unit, Hefei, China

3 The Key Laboratory of Anti-Inflammatory and Immune Medicine, Anhui Medical University, Ministry of Education, Hefei, China

microbial pathogens, and involves the activation of the multi-protein complex known as the inflammasome [18, 19]. The inflammasome is a large multi-protein complex located in the cytoplasm. Its main function is to activate caspase-1 and further promote the cleavage and maturity of the proinflammatory cytokine IL-1β/18 [20, 21]. The inflammasome consists of three proteins, including receptor proteins, apoptosis-associated speck-like protein (ASC) and effect molecule pro-caspase-1 [22]. Depending on the type of receptor protein, inflammasomes are classified into four categories: NLRP1 [23], NLRP3 [24], and NLRC4 [25] and the AIM2 [26, 27] inflammasome. The classical signalling pathway of pyroptosis mediated by caspase-1 is activated in cells exposed to ATP, uric acid crystallisation, dsDNA, alum, Ca^{2+}, bacterial toxins and H^+ [28–31].

Pyroptosis is closely related to the development of many complex diseases, such as bacterial infection, atherosclerotic disease and some neurological systemic diseases [32, 33]; and also contributes to some autoimmune diseases, such as RA [34, 35], suggesting that pyroptosis may be involved in the development of RA. Furthermore, extracellular acidosis induces the synthesis and secretion of the proinflammatory cytokine IL-1β in macrophages via the upregulation of the expression of the NLRP3 inflammasome [36] and extracellular acidosis induced the synthesis of the proinflammatory cytokine IL-1β and lead to pyroptosis [37].

Acid-sensitive ion channels (ASICs) represent classes of extracellular acidosis-activated cation channels belonging to the degenerin/epithelial Na^+ channel family [38]. Thus far, ASICs have been found to be widely distributed in the central and peripheral nervous systems. ASICs consists of seven members, ASIC1a, 1b, 1b2, 2a, 2b, 3 and 4, encoded by four homologous genes [39–41]. ASIC1a is a unique subunit that transports calcium ions, while the other ASICs influence only sodium ions [42]. Various pathological conditions, such as inflammation, ischaemia, tumours and epilepsy, are related to the activation of ASIC1a [43, 44], suggesting that ASIC1a broadly participates in pathophysiological processes in individuals.

Our previous study indicated that ASIC1a, 2a and 3 are present in articular chondrocytes in rats, and that these proteins are upregulated in chondrocytes in rats with adjuvant arthritis. Furthermore, ASIC1a mediates chondrocyte apoptosis induced by extracellular acidosis by increasing intracellular $[Ca^{2+}]_i$ [39]. Apoptosis occurs in articular chondrocytes in RA, and blocking ASIC1a by amiloride reduced apoptosis in articular chondrocytes induced by extracellular acidosis [40].

In summary, it has already been determined that apoptosis in chondrocytes occurring in RA is accompanied by the release of large amounts of proinflammatory cytokines. Extracellular acidosis (pH 6.0) can significantly induce apoptosis in articular chondrocytes in a pH-dependent manner. These phenomena are consistent with the features of pyroptosis, but whether chondrocyte pyroptosis is involved in the course of RA remains unclear.

In this study, we investigated the role of Ca^{2+} in ASIC1a-mediated chondrocyte pyroptosis in AA rats both in vivo and in vitro. First, we investigated pyroptosis in chondrocytes in AA rats and then observed the effects of ASIC1a on pyroptosis in chondrocytes by blocking ASIC1a. In vitro, we induced extracellular acidosis to simulate the microenvironment of chondrocytes in RA and studied the possible mechanism.

Materials and methods

Construction of an adjuvant arthritis model and administration

All experiments were approved by Anhui Medical University, and the methods were carried out in accordance with the relevant guidelines and regulations. All animals were cared for in compliance with the guidelines for Animal Care and Use of Laboratory Animals set by the Association of Laboratory Animal Sciences and the Center for Laboratory Animal Sciences at Anhui Medical University.

Forty young adult male Sprague–Dawley (SD) rats weighing 160–180 g were randomly divided into four groups (the normal group, model group, aspirin group and amiloride group). The AA rat model was established by an intradermal injection of 100 μl of Freund's complete adjuvant (20 mg/ml) into the left hind paw. The volume of the right hind paws of the rats was measured on day 0, day 10, day 14, day 21 and day 28 to assess inflammation in the AA rats. The rats in the aspirin group received aspirin (50 mg/kg, sigma) by gavage once a day, the rats in the amiloride group received an intraperitoneal injection of amiloride (100 mg/kg, sigma) once a day, and the rats in the model group received an intraperitoneal injection of normal saline as a control during the third week after modelling. All rats were sacrificed on day 28. The plasma of the rats was collected for the detection of the proinflammatory cytokines IL-1β/18. The ankle joints were collected for HE staining and immunohistochemistry, and the hind knee joints were prepared for the extraction of the total protein and RNA from the articular cartilage.

Ankle histopathological examination

The ankle joints were fixed with 4% paraformaldehyde for 48 h, followed by decalcification with 10% EDTA solution for 2 months. The tissues were dehydrated, embedded in paraffin and cut into thick slices (5–7 μm). The slices were stained with haematoxylin and eosin staining dyes. The

pathological changes in the ankle were observed under an inverted microscope.

Immunohistochemistry of type II collagen (Col 2a) in the ankle cartilage

The tissue slices were obtained as previously described, and the expression levels of Col 2a in the ankle cartilage was assessed by immunohistochemistry staining. The steps were performed in accordance with the instructions of the SP immunohistochemical kits (Zhongshan Jinqiao, China). The microscope photographs were analysed by Image-Pro.

Isolation and culture of primary articular chondrocytes

Articular chondrocytes were obtained from young male SD rats as previously described [39]. The knee cartilage was cut into small pieces (1 mm^3) and then incubated with trypsin solution for 30 min, followed by incubation with type II collagenase (0.2%) for 3 h After digestion, the free cells were centrifuged for 5 min at 1000 rpm and resuspended in phosphate buffered saline (PBS). The fresh free cells were plated at a density of 2×10^4 cells/well in plates that had been previously immersed in plastic dishes filled with culture medium (DMEM supplemented with 2 mM glutamine, 100 IU/ml penicillin, 100 μg/ml streptomycin and 10% FBS). The chondrocytes were cultured at 37 °C in an environment with 5% CO_2 for 2 days. The supernatant was replaced with fresh medium after the cells had adhered completely. All chondrocytes were third to fourth generation.

Reverse transcription and real-time PCR

The primary articular chondrocytes were transfected with ASIC1a shRNA (Forward:5′-CACCGCCAAGAAGTTCA ACAAATCGTTCAAGAGACGATTTGTTGAACTTCTT GGCTTTTTTG-3′; Reverse:5′-GATCCAAAAAAGCCAA GAAGTTCAACA AATCGTCTCTTGAACGATTTGTTG AACTTCTTGGC-3′) or pre-incubated with the ASIC1a specific inhibitor Pctx-1 (100 ng/ml, Phoenix Pharmaceuticals) and Calcium chelator BAPTA-AM (10 μM, TOCRIS) for 1 h, followed by adjustment of the cell culture medium pH to 6.0 for 48 h. The chondrocytes were lysed by TRIzol reagent, and the total RNA was extracted by Chloroform. The total RNA (1 μg) was reverse transcribed into cDNA according to the manual instructions of the TAKARA kit, and the cDNA was used for the real-time polymerase chain reaction (PCR) process. The real-time PCR primer sequences for ASIC1a, caspase-1, ASC, NLRP3, IL-1β, IL-18 and β-actin were designed as follows (Table 1). The primers were all designed and synthesised by Shanghai Biology Engineering Corporation. The total volume of the real-time PCR reaction system was 10 μl, including 0.3 μl of the primers for the upstream and downstream genes, followed by the addition of 5 μl SYBR Green and 3.9 μl enzyme-free water. Finally, 0.5 μl cDNA were added to the mixture. The cDNA was first incubated for 10 min at 95 °C, followed by the cycle conditions of denaturation at 95 °C for 15 s, annealing at 60 °C for 30 s, and extension at 72 °C for 30 s. The system automatic amplification cycles were set to 40 cycles for each primer. The entire process was conducted with Piko Real Software of Thermo.

Table 1 Primer sequences of several genes for real-time PCR

Gene	Sequences	Length (bp)
ASC	F:5′-TTATGGAAGAGTCTGGAGCTGTGG-3′	101
	R:5′-AATGAGTGCTTGCCTGTGTTGG-3′	
NLRP3	F:5′-CAGACCTCCAAGACCACGACTG-3′	127
	R:5′-CATCCGCAGCCAATGAACAGAG-3′	
Caspase-1	F:5′-TGCCTGGTCTTGTGACTTGGAG-3′	133
	R:5′-ATGTCCTGGGAAGAGGTAGAAACG-3′	
IL-1β	F:5′-CTCAACTGTGAAATAGCAGCTTTC-3′	110
	R:5′-GGACAGCCCAAGTCAAGG-3′	
IL-18	F: 5′-ATATCGACCGAACAGCCAAC-3′	105
	R:5′-TTCCATCCTTCACAGATAGGG-3′	
ASIC1a	R:5′-GGCCAACTTCCGTAGCTTCA-3′	67
	R:5′-ATGCCCTGCTCTGTCGTAGAA-3′	
β-actin	F:5′-GGAGATTACTGCCCTGGCTCCTA-3′	150
	R:5′-GACTCATCGTACTCCTGCTTGCTG-3′	

Western blotting

The primary articular chondrocytes were pre-incubated as previously described. The total protein was extracted from a cell using RIPA protein lysates (150 mmol/l NaCl, 1.0% Nonidet P-40, 0.5% deoxycholate, 0.1% sodium dodecylsulfate (SDS), 50 mmol/l Tris and pH 8.0), and the supernatant of the mixture from each group was quantified by a fluorescent protein quantitative instrument (NanoDrop 2000, Thermo). The total protein samples from each group were separated by 10% SDS polyacrylamide gel electrophoresis and then blotted onto a polyvinylidene difluoride (PVDF) membrane. The membrane was incubated with 5% skim milk for 3 h and then probed with specific primary affinity-purified antibodies against ASIC1a (Alomone Labs,1:1000), caspase-1 p10 (Bioss,1:500), ASC (Bioss,1:500), NLRP3 (Bioss,1:500), Agg (Cell Signalling Technology,1:1000), Col 2a (Bioss,1:500) and β-actin (Bioss,1:500) overnight, followed by incubation with secondary antibodies for 1 h. The PVDF membrane was

exposed and photographed using a chemiluminescence ECL kit.

Immunofluorescence of ASC and NLRP3

The primary articular chondrocytes were stimulated by pH 6.0 with or without Pctx-1 and BAPTA-AM once the cell density reached 60–70%. The cells were fixed with acetone for 15 min, followed by incubation with Triton X-100 (0.3% in PBS) for 15 min and H_2O_2 (3% in PBS) for 15 min to clear the effect of endogenous peroxidase. Furthermore, the cells were incubated with bovine serum albumin (5% in PBS) for 30 min at room temperature to fix the sites and overnight with ASC and NLRP3 antibodies diluted to 1:200. PBS served as a negative control instead of the primary antibody. After probing, the cells were incubated with a fluorescent secondary antibody (1:200) in the dark for 30 min and dyed with DAPI solution. The microscope photographs were analysed by Image-Pro.

Enzyme-linked immunosorbent assay (ELISA) of IL-1β and IL-18

The primary articular chondrocytes were pre-incubated as previously mentioned. The cell culture media were collected and centrifuged at 1000×*g* for 20 min to remove cell debris and impurities. Rat plasma obtained from the in vivo experiment was centrifuged at 1000×*g* for 15 min within 20 min of the sample collection. The IL-1β/18 enzyme-linked immunosorbent assay (ELISA) process was performed in accordance with the users' operating instruction procedures by Elab Science. The determination of the optical density value of each well was conducted with a microplate reader set to 450 nm, and the absorbance was set into the standard curve to calculate the content of the proinflammatory cytokines IL-1β/18.

Lactate dehydrogenase (LDH) release assay

The lactate dehydrogenase (LDH) assessment process was performed in accordance with the users' operating instruction procedure of the LDH Cytotoxicity Detection Kit by Beyotime Biotechnology. The 96-well cell culture plate was divided into negative control wells, the largest activity wells and drug treatment wells. The chondrocytes in the drug treatment wells were pre-incubated as previously described. The LDH release agent (20 µl) was added to the largest activity wells 1 h before the scheduled time and cultured in an incubator for 1 h. The cell plate was centrifuged at 400×*g* for 5 min, and then, 120 µl of the supernatant were transferred to a new, fresh 96-well plate, followed by the detection of the absorbance at 490 nm by a full wavelength microplate reader.

AO/EB staining

The AO and EB powders were dissolved to 100 µg/ml with PBS buffer to prepare the stock solutions and mixed in equal parts before the experiment. Primary articular chondrocytes were seeded on slips that were sterile and clean and then pre-incubated as previously described. The slips were washed twice with PBS buffer, and the AO/EB staining dye working solution was added to the slips for 15 s. The death rate of the chondrocytes was observed, and the chondrocytes were photographed under a fluorescence inverted microscope. The microscope photographs were analysed by Image-Pro.

Laser scanning confocal microscopy for intracellular calcium

The primary articular chondrocytes were pre-incubated and intracellular calcium imaging was performed as previously described [45]. The cells were incubated with 4 µM Fluo-3-AM and 0.02% Pluronic F-127 (Biotium) for 30 min at 37 °C. The fluorescence of intracellular Fluo-3 was quantitated by confocal laser scanning fluorescence microscopy (Zeiss). After recording the basic fluorescence intensity for approximately 100 s, the acidic solution (pH 6.0) was added directly with a pipette far from the recorded cells. The recording continued throughout the continued addition of the acidic solution and lasted for approximately 10 min. Each time, seven cells were measured, and the mean value of the fluorescence of each cell was calculated. The intensity of the fluorescence of individual cells was measured using LSM 5 Image software.

Statistics

The results of the study are expressed as the means ± SEM of three independent experiments. The analyses of the data obtained from the different treatment groups were completed with a single factor analysis of variance (ANOVA). P values < 0.05 were considered significant.

Results

Amiloride ameliorated and inhibited pyroptosis in the articular cartilage

Figure 1a shows that the AA model was successfully established by day 14. The paws and ankle joints of the AA rats were significantly swollen compared with normal rats, and the generation of rheumatoid nodules was observed in their tails. As shown in Fig. 1b, c, significant articular changes, including hyperplasia of the synovium,

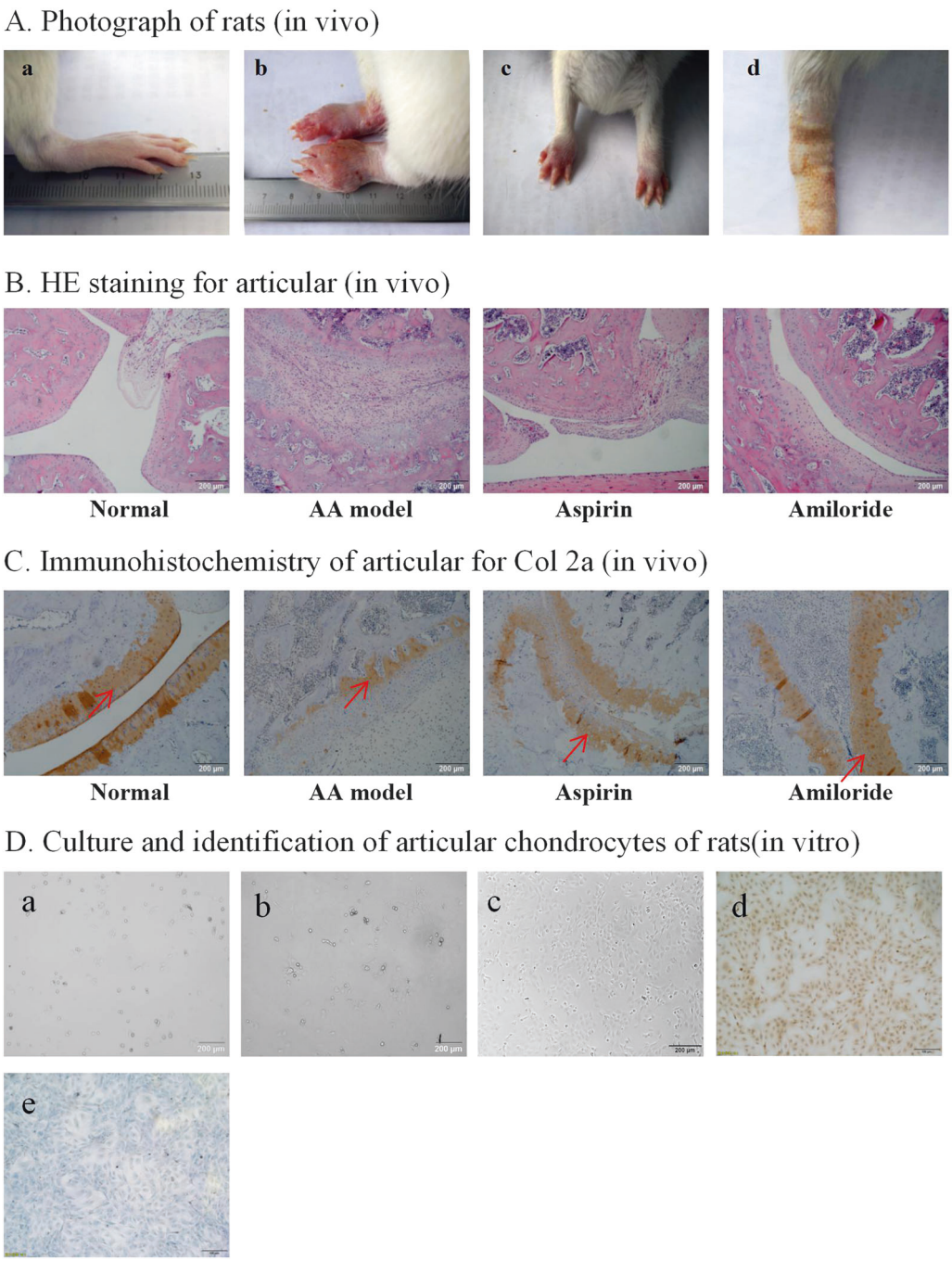

Fig. 1 Effects of amiloride on AA progression and the identification of primary rat articular chondrocytes. **a** Photograph of rats on day 14; **b** Amiloride inhibited the pathological changes in articular tissues from AA rats as observed by HE staining; **c** Amiloride inhibited the expression of type 2 collagen as observed by immunohistochemistry. **d** Isolation, culture and identification of primary rat articular chondrocytes (a, b primary articular chondrocytes isolated after 2 and 4 days. c Primary articular chondrocytes covered the bottom fully; d, e chondrocytes identified by Col 2a and Agg staining)

thickening of the lining layer, formation of pannus and infiltration of a variety of inflammatory cells, were observed in the AA rats. In addition, rats treated with the classic nonsteroidal anti-inflammatory drug aspirin (50 mg/kg) and the ASIC1a inhibitor amiloride (100 mg/kg) improved prognoses in terms of the pathological articular changes and upregulation of articular cartilage matrix Col 2a.

Figure 2 illustrates pyroptosis in the articular chondrocytes in the AA model. Figure 2a shows that the mRNA of ASIC1a, ASC, NLRP3, caspase-1 and the proinflammatory cytokines IL-1β and IL-18 sufficiently

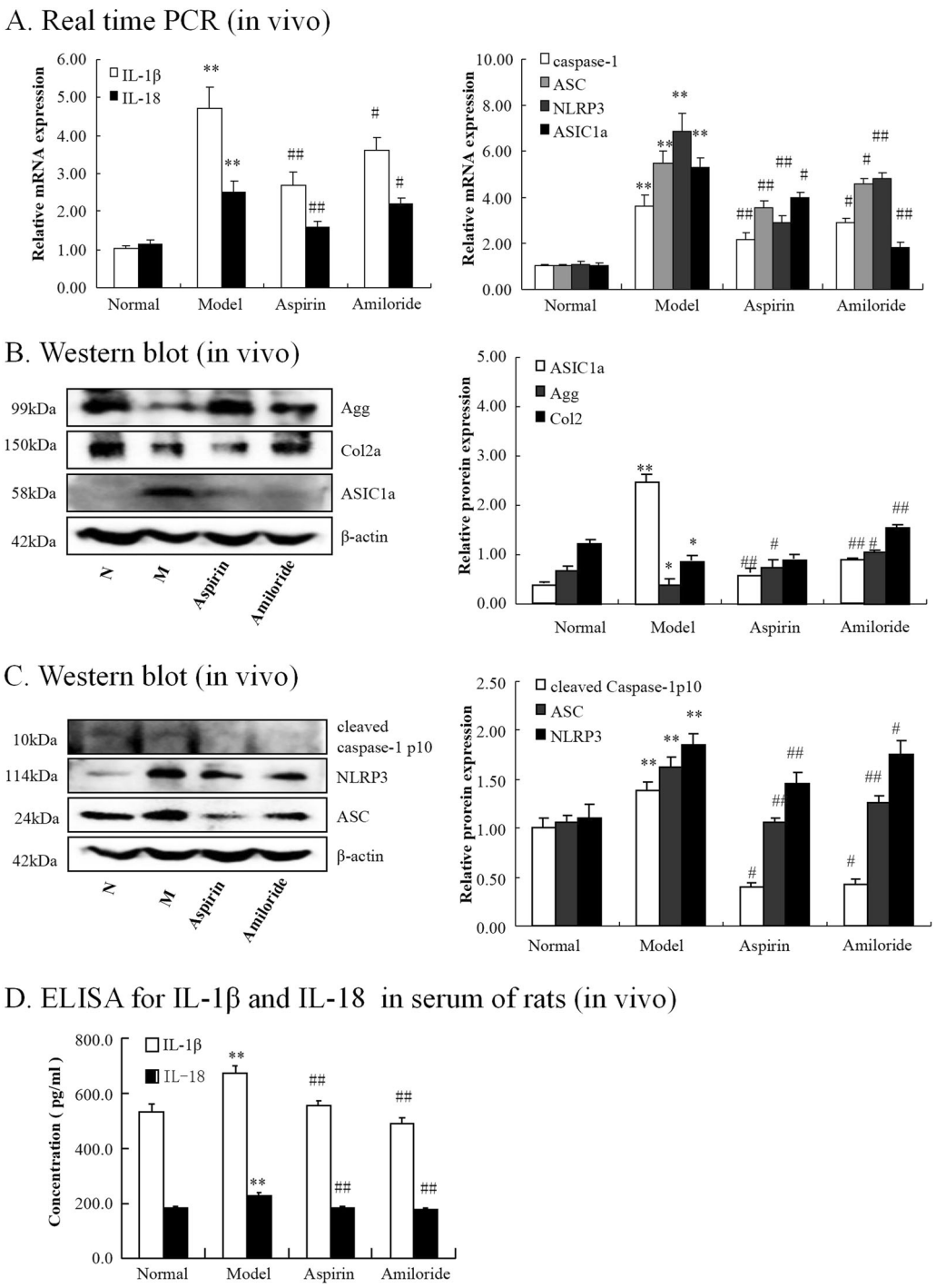

Fig. 2 Amiloride inhibited pyroptosis in articular chondrocytes in AA rats. **a** Amiloride attenuated the mRNA expression of ASC, NLRP3, caspase-1, IL-1β, IL-18 and ASIC1a by real-time PCR in articular cartilage tissues. **b** Amiloride attenuated the protein expression of Agg, Col2a and ASIC1a by western blotting. **c** Amiloride attenuated the protein levels of ASC, NLRP3 and cleaved caspase-1 p10. **d** Amiloride downregulated the levels of IL-1β and IL-18 by ELISA in the plasma of rats. The data are presented as the mean ± SEM of five rats, $^{*}P < 0.05$, $^{**}P < 0.01$ vs. normal group; $^{\#}P < 0.05$, $^{\#\#}P < 0.01$ vs. model group

increased in the tissues obtained from the AA rats' articular cartilage, but in the aspirin- and amiloride-treated groups, the upregulation of these genes was repressed. We then studied the effects of amiloride on the protein expression of pyroptosis-related proteins and components of the articular cartilage extracellular matrix, i.e., Agg and Col 2a. The results (Fig. 2b, c) demonstrate that Agg and Col 2a decreased sharply under the AA conditions, but aspirin and amiloride reversed the degeneration of these two proteins. Western blotting of ASC, NLRP3, caspase-1p10 and

ASIC1a showed similar trends. The results of ELISAs for IL-1β and IL-18 (Fig. 2d) in the plasma from the four groups of rats showed that the AA rats had a higher level of the proinflammatory cytokines IL-1β and IL-18 than the rats in the normal group, but that aspirin and amiloride could suppress these effects.

Isolation, culture and identification of rat articular chondrocytes

The primary articular chondrocytes were obtained as previously described. After extraction, the cells were round and adhered to the bottom of the plate after 48 h (Fig. 1d, panel a). Initially, the chondrocytes proliferated slowly (Fig. 1d, panel b), but after 7 days of culture, the chondrocytes were confluent (Fig. 1d, panel c). The extracellular space stained positive for Col 2a and Agg, indicating that the isolated cells were indeed primary articular chondrocytes.

Extracellular acidosis induced pyroptosis in primary articular chondrocytes

Other studies have indicated that extracellular acidosis promotes the secretion of the proinflammatory cytokines L-1β and IL-18 in macrophages by inducing the expression of the NLRP3 inflammasome. We stimulated primary articular chondrocytes with several pH levels, including pH 6.0, for different times to observe pyroptosis in the primary articular chondrocytes. Figures 3a, 4a show that extracellular acidosis could increase the protein expression of ASC, NLRP3, cleaved caspase-1p10 and ASIC1a and that stimulation with pH 6.0 generated significant effects (Fig. 3b). The results of the real-time PCR analysis of ASC, NLRP3 and caspase-1 showed the same phenomenon as the western blotting results (Fig. 3c), ELISA results of the expression of IL-1β/IL-18 in the culture medium (Fig. 3d) and the results of the real-time PCR analysis of the mRNA expression of IL-1β/IL-18 in the primary articular chondrocytes (Fig. 3e). The level of LDH was a secondary indicator of pyroptosis. Figure 4b shows that acidosis can induce the release of LDH in a time-dependent manner at a pH of 6.0.

Construction of an ASIC1a knock-down model of chondrocytes

An ASIC1a shRNA sequence was designed and synthesised by Shanghai Biology Engineering Corporation and then transfected into primary articular chondrocytes according to standard operating procedures. We found that ASIC1a shRNA could be successfully transfected into chondrocytes (Fig. 4c). The mRNA and protein expression of ASIC1a was significantly decreased after transfection with ASIC1a shRNA (Fig. 4d, e), but the empty vector had no effect.

Role of ASIC1a in extracellular acidosis-induced pyroptosis in primary articular chondrocytes

Previous studies have reported that ASIC1a influences Ca^{2+} permeability, and increasing intracellular $[Ca^{2+}]_i$ significantly activates the pyroptosis-associated pathway. Therefore, we investigated the effects of ASIC1a on extracellular acidosis-induced pyroptosis in primary articular chondrocytes. Figures 5a, 6b show that the ASIC1a-specific inhibitor Pctx-1 and ASIC1a shRNA attenuated extracellular acidosis-induced pyroptosis in primary articular chondrocytes through the detection of ASC, NLRP3 and cleaved caspase-1p10. The gene expression levels of ASC, NLRP3, caspase-1, IL-1β and IL-18 (Fig. 5b) and the expression levels of IL-1β and IL-18 in the culture medium were decreased by pre-incubation with Pctx-1 and transfection with ASIC1a shRNA (Fig. 5c). The LDH level in the culture medium of the primary articular chondrocytes (Fig. 5d) was suppressed by Pctx-1. Cells positive for AO/EB staining are also secondary indicators of pyroptosis. Figure 6a shows that the chondrocytes in the pH 7.4 group were mostly dyed green, and the chondrocytes in the pH 6.0 group were mainly stained orange, but Pctx-1 could suppress these effects. These findings indicate that extracellular acidosis can successfully induce pyroptosis in primary articular chondrocytes and that the inhibition of ASIC1a has a beneficial effect.

We investigated the changes in $[Ca^{2+}]_i$ in articular chondrocytes treated with extracellular acidosis. Based on the confocal micrographs (Fig. 6c, panels a–c) and representative traces, the application of extracellular acidosis (pH 6.0) significantly increased $[Ca^{2+}]_i$ in the articular chondrocytes. The ASIC1a-specific inhibitor Pctx-1 reduced the amplitude of the $[Ca^{2+}]_i$ response to extracellular acidosis. Therefore, extracellular acidosis-induced pyroptosis in primary articular chondrocytes may be relevant to *ASIC1a-mediated* $[Ca^{2+}]_i$.

Role of Ca^{2+} in ASIC1a-mediated extracellular acidosis-induced pyroptosis in primary articular chondrocytes

As previously mentioned, the concentration of intracellular Ca^{2+} is closely associated with pyroptosis in cells. We investigated whether the increasing intracellular Ca^{2+} concentration was important for ASIC1a-mediated extracellular acidosis-induced pyroptosis in primary articular chondrocytes. Chelating agents, such as Ca^{2+} BAPTA-AM, can attenuate extracellular acidosis-induced pyroptosis in primary articular chondrocytes based on the expression of ASC, NLRP3 and cleaved caspase-1p10 (Fig. 7a, f). BAPTA-AM also had a negative effect on the concentrations of IL-1β and IL-18 in the culture medium and the mRNA expression levels of ASC, NLRP3, caspase-1, IL-1β

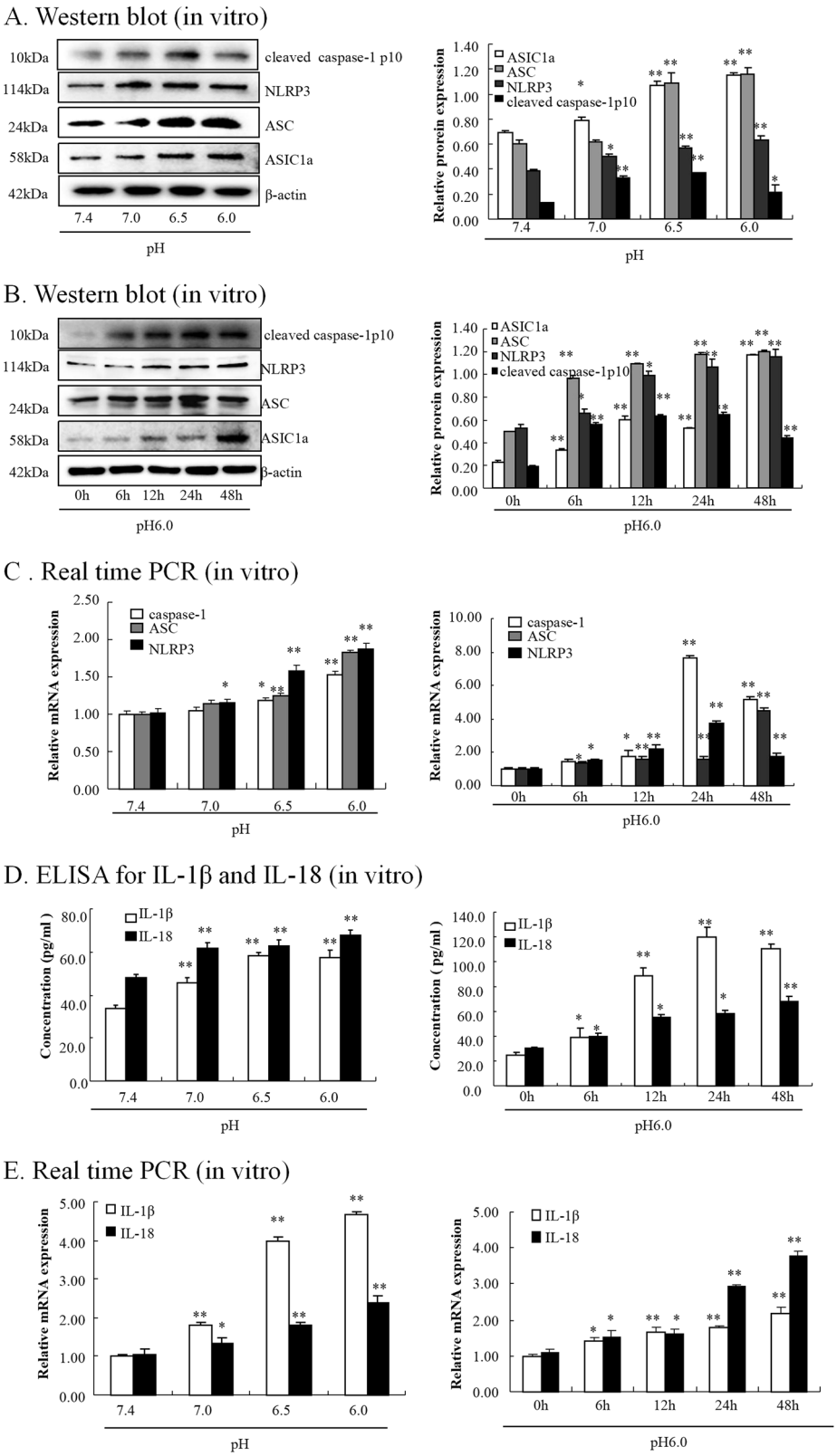

Fig. 3 Effects of extracellular acidosis on pyroptosis in primary articular chondrocytes. **a** The effects of treatment with several pH levels on the protein levels of ASC, NLRP3, cleaved caspase-1p10 and ASIC1a. **b** The effects of pH 6.0 stimulation on the protein levels of ASC, NLRP3, cleaved caspase-1p10 and ASIC1a. **c** Real-time PCR analysis of ASC, NLRP3 and caspase-1 in primary articular chondrocytes. **d** Extracellular acidosis induced the expression of IL-1β and IL-18 in culture medium by ELISA. **e** Extracellular acidosis induced the mRNA expression of IL-1β and IL-18. The data are presented as the mean ± SEM of three wells in three independent experiments, $^{*}P < 0.05$, $^{**}P < 0.01$ vs. pH 7.4 group

and IL-18 by real-time PCR (Fig. 7b, c). Moreover, BAPTA-AM could exclude the primary articular chondrocytes from extracellular acidosis-induced pyroptosis (Fig. 7d). The primary articular chondrocytes co-incubated with pH 6.0 and BAPTA-AM exhibited inhibition of extracellular acidosis-induced pyroptosis by AO/EB

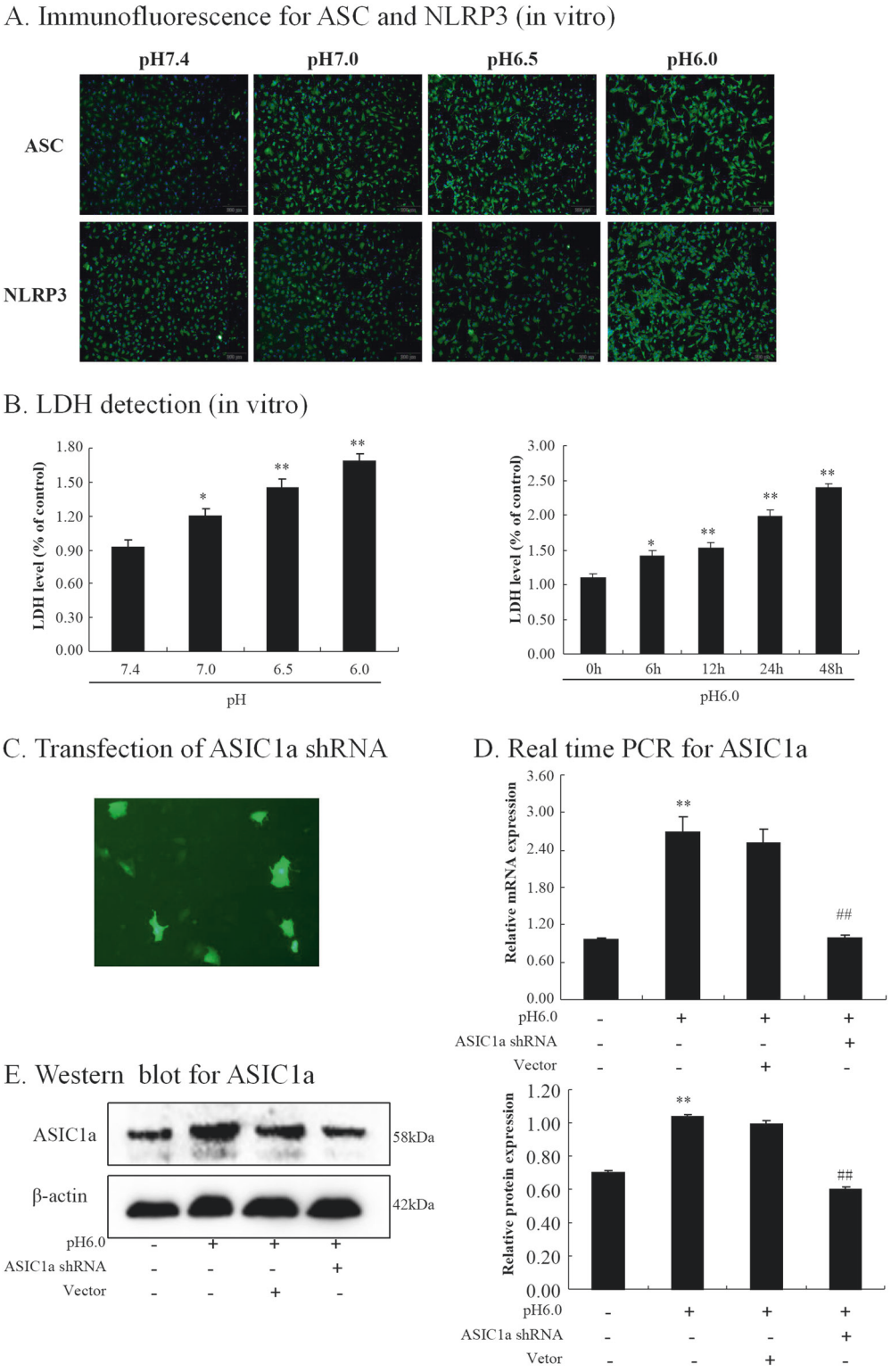

Fig. 4 Effects of extracellular acidosis on pyroptosis in primary articular chondrocytes and the construction of the ASIC1a knock-down model. **a** Extracellular acidosis induced the expression of ASC and NLRP3 by immunofluorescence. **b** Extracellular acidosis induced the release of LDH. **c** Photographs of chondrocytes after transfection with ASIC1a shRNA; **d**, **e**. ASIC1a shRNA inhibits the mRNA and protein expression of ASIC1a. The data are presented as the mean ± SEM of three wells in three independent experiments, $^{*}P < 0.05$, $^{**}P < 0.01$ vs. pH 7.4 group; $^{\#}P < 0.05$, $^{\#\#}P < 0.01$ vs. pH 6.0 group

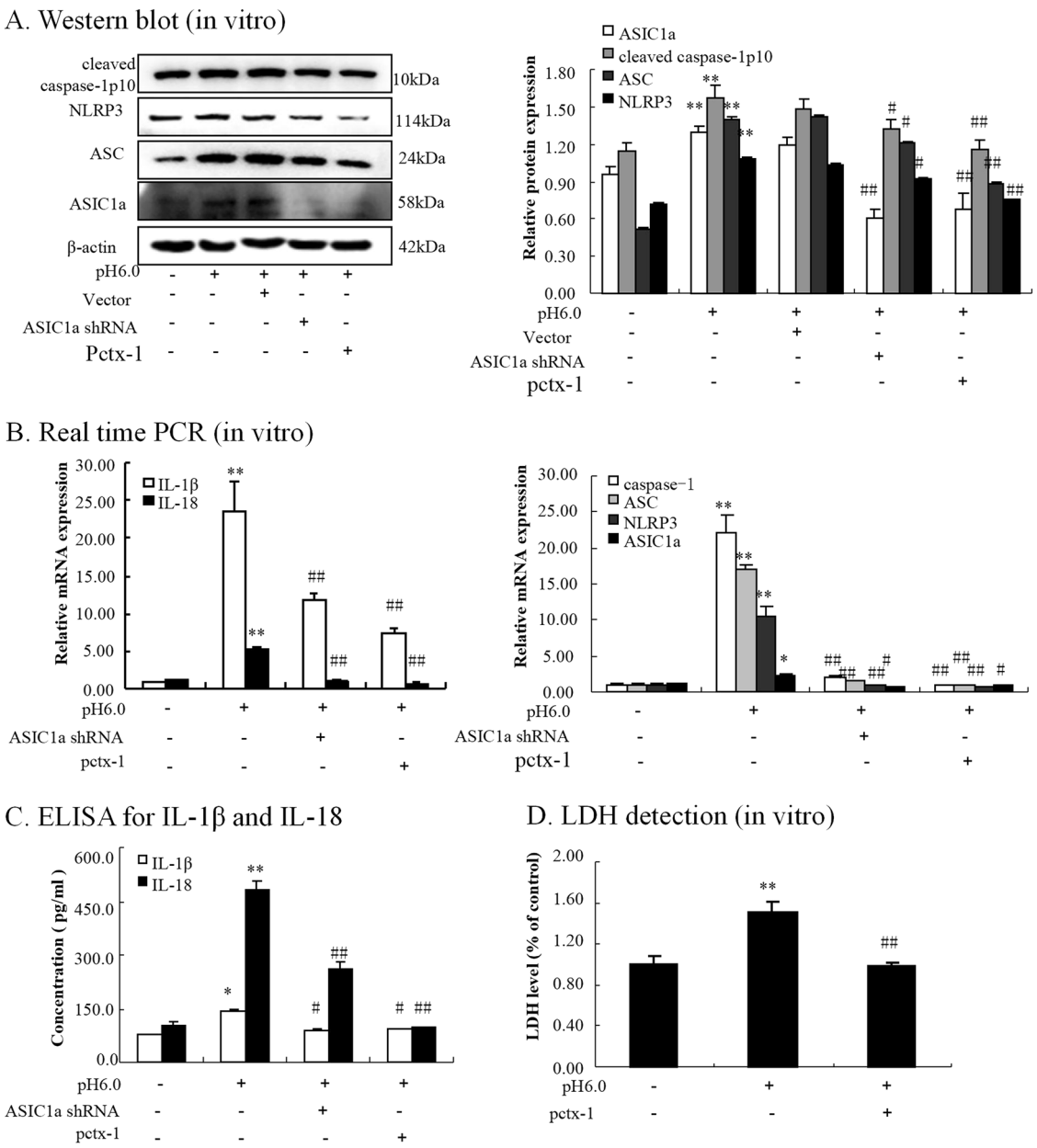

Fig. 5 Activation of ASIC1a promoted extracellular acidosis-induced pyroptosis in primary articular chondrocytes. **a** ASIC1a-specific inhibitor Pctx-1 and ASIC1a shRNA attenuated extracellular acidosis-induced pyroptosis in primary articular chondrocytes by western blotting for ASC, NLRP3 and cleaved caspase-1p10. **b** The negative effects of Pctx-1 and ASIC1a shRNA on extracellular acidosis-induced pyroptosis in primary articular chondrocytes. **c** Pctx-1 and ASIC1a shRNA attenuated the levels of IL-1β and IL-18 in culture medium. **d** Pctx-1 suppressed the release of LDH in primary articular chondrocytes. The data are presented as the mean ± SEM of three wells in three independent experiments, $^{*}P < 0.05$, $^{**}P < 0.01$ vs. pH 7.4 group; $^{\#}P < 0.05$, $^{\#\#}P < 0.01$ vs. pH 6.0 group

staining (Fig. 7e). In summary, ASIC1a mediates extracellular acidosis-induced pyroptosis in primary articular chondrocytes possibly by regulating $[Ca^{2+}]_i$.

Discussion

Several genetic and environmental factors have been implicated in the development of RA [46, 47], eventually leading to the erosion of the articular cartilage. Other studies have indicated that significant apoptosis occurs in articular chondrocytes during RA, suggesting that the death of articular chondrocytes plays a critical role in the progression of RA. One study showed that the proinflammatory cytokines IL-1β, IL-6 and IL-18 [7] play a vital role in the destruction of articular cartilage and chondrocyte apoptosis; levels of the proinflammatory cytokines IL-1β and IL-18 were significantly increased in

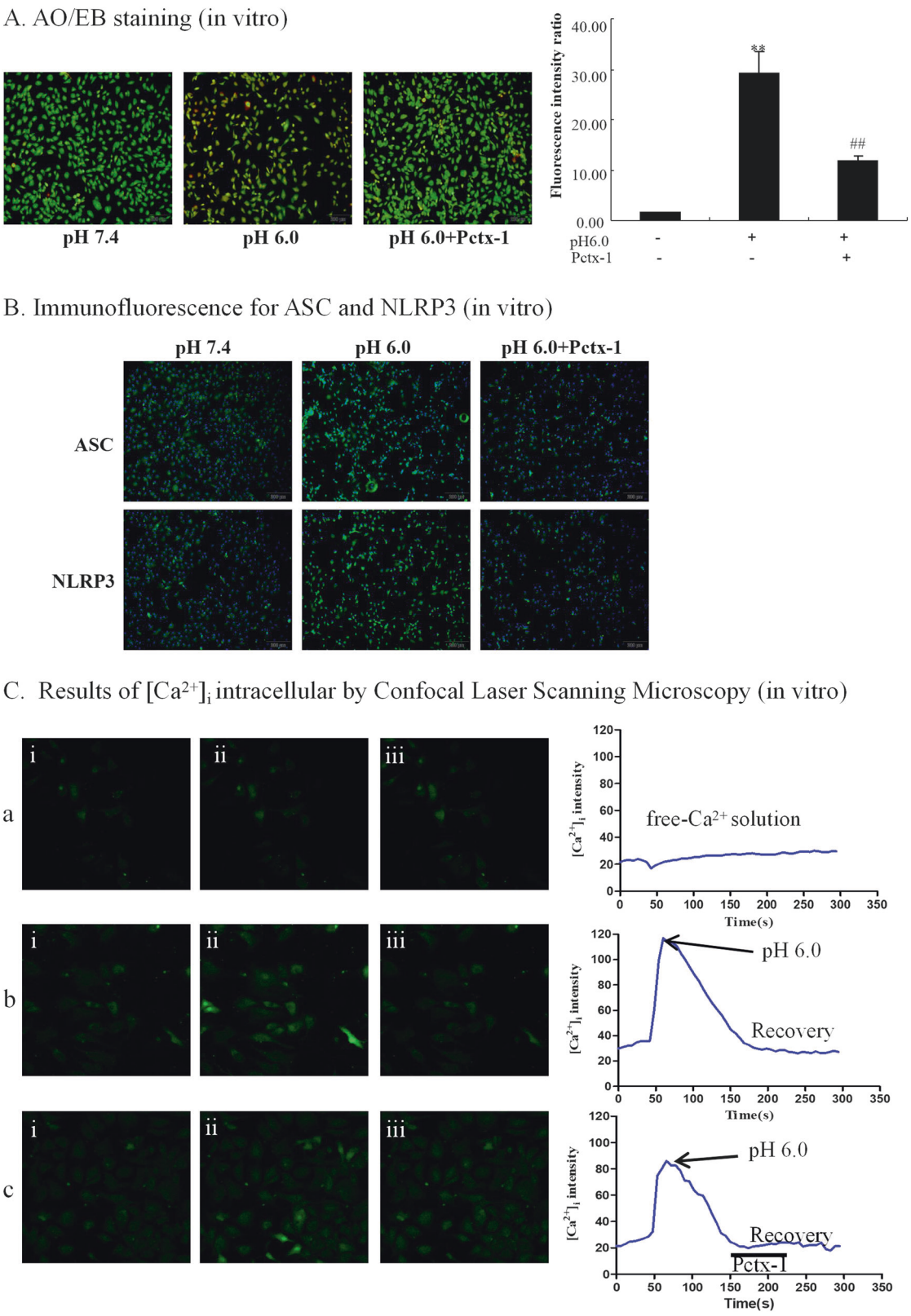

AA rats' plasma and that extracellular acidosis induced the synthesis of the proinflammatory cytokines IL-1β and IL-18 in primary chondrocytes. The expression levels of Col 2 and Agg sharply decreased in the articular cartilage of the AA rats. This finding is consistent with a previous study that showed that articular chondrocytes could

◀ **Fig. 6** Activation of ASIC1a promoted extracellular acidosis-induced pyroptosis in primary articular chondrocytes and the upregulation of intracellular $[Ca2+]_i$. **a** Pctx-1 inhibited pyroptosis induced by extracellular acidosis in primary articular chondrocytes by AO/EB staining, semi-quantitative results. **b** Pctx-1 downregulated the expression of ASC and NLRP3 in primary articular chondrocytes by immunofluorescence. **c** Pctx-1 downregulates intracellular $[Ca^{2+}]_i$ by laser scanning confocal microscopy. The data are presented as the mean ± SEM of three wells in three independent experiments, $^{*}P < 0.05$, $^{**}P < 0.01$ vs. pH 7.4 group; $^{\#}P < 0.05$, $^{\#\#}P < 0.01$ vs. pH 6.0 group

secrete the proinflammatory cytokines IL-1, IL-8 and IL-18 during osteoarthritis [48].

Recent studies have demonstrated that the incidence of pyroptosis in several types of cells plays a crucial role in the pathogenesis of RA [49, 50], suggesting that pyroptosis and the inflammasome may be involved in the development of RA. The NLRP3 and NLRP1 inflammasomes, rather than the NLRC4 inflammasome, were associated with the development of RA [51, 52]. Under pathological conditions, pyroptosis require two signals for the assembly of the inflammasome and the activation of caspase-1 [53]. The first signal promotes the expression of genes and proteins that are components of the inflammasome and proinflammatory cytokine precursors under stress states. The second signal can promote the assembly of the inflammasome complex and cleave the proinflammatory cytokine precursors into their mature forms [54]. Ca^{2+} and H^{+} can both efficaciously activate the NLRP3 inflammasome, which is attributed to the release of the proinflammatory cytokines IL-1β and IL-18.

A gene polymorphism in the NLRP3 inflammasome was detected in a Swedish population of RA patients [33], and the expression of the NLRP3 inflammasome was shown to be significantly increased in their peripheral blood cells. Another study found that the inhibition of the NLRP3 inflammasome by A20 has a protective effect in RA patients. Cell pyroptosis occurs in RA [35], but the specific mechanism remains unclear. The low pH of joint fluid is a main pathogenic feature of RA. Our study indicates that AA rats express high levels of the components of the NLRP3 inflammasome (ASC, NLRP3 and caspase-1). The conventional anti-RA drug aspirin reversed the increase in expression of the inflammasome proteins IL-1β and IL-18 and also suppressed the degeneration of articular cartilage Col 2a, which had a protective effect in RA patients. Thus, articular chondrocyte pyroptosis occurs during AA progession, and the conventional anti-RA drug aspirin inhibits pyroptosis in chondrocytes. Moreover, extracellular acidosis upregulated the expression of the components of the NLRP3 inflammasome (ASC, NLRP3, and caspase-1), IL-1β and IL-18. The cells showed positive results after AO/EB staining, and the release of LDH was upregulated.

Our previous study also found that pH 6.0 acidosis treatment could significantly induce apoptosis in articular chondrocytes. Studies have suggested that extracellular acidosis increases the concentration of intracellular Ca^{2+} by activating ASIC1a. We speculate that ASIC1a plays a critical role in pyroptosis in chondrocytes during the process of RA and that Ca^{2+} participates in the mediation of pyroptosis. The results of our study show that the inhibitor of ASIC1a amiloride reversed the increase in expression of ASIC1a, inflammasome proteins, IL-1β and IL-18. We also found that amiloride suppressed the degeneration of articular cartilage Col 2a, which has a protective effect in RA patients.

In order to determine the mechanisms of ASIC1a-mediated pyroptosis in chondrocytes in AA rats, we incubated primary articular chondrocytes at pH 6.0 to simulate the microenvironment of articular chondrocytes and then induced stimulation with Pctx-1 to explore the effects of ASIC1a on pyroptosis in chondrocytes. We found that the cells stimulated by pH 6.0 showed high expression of ASIC1a, the components of the NLRP3 inflammasome, and IL-1β and IL-18. The cells also stained positive for AO/EB, and LDH was upregulated. Furthermore, Pctx-1 reversed the effects of extracellular acidosis on primary articular chondrocytes.

ASIC1a mediates Ca^{2+} permeability and that intracellular $[Ca^{2+}]_i$ is closely linked to pyroptosis in cells as previously mentioned. We investigated whether increasing intracellular $[Ca^{2+}]_i$ mediated by ASIC1a is associated with acidosis-induced pyroptosis in primary articular chondrocytes. We found that the chelating agent Ca^{2+} BAPTA-AM could suppress pyroptosis induced by acidosis in primary articular chondrocytes. Overall, ASIC1a mediates extracellular acidosis-induced pyroptosis in primary articular chondrocytes, and Ca^{2+} is associated with this process.

In summary, the intra-articular accumulation of inflammatory metabolites results in a decrease in the pH of joint fluid and activates ASIC1a, which promotes Ca^{2+} flow into cells. The upregulation of intercellular $[Ca^{2+}]_i$ contributes to the expression, aggregation and assembly of the NLRP3 inflammasome, followed by the activation of caspase-1, whose main function is to cleave pro-IL-1β and pro-IL-18 into their biologically active forms. Although Ca^{2+} is associated with ASIC1a-mediated pyroptosis in primary articular chondrocytes, other specific mechanisms may be involved in the process. Nonetheless, we conclude that this study indicates that it may be possible to devlop effective drugs for RA that target the inhibition of pyroptosis and IL-1β/18.

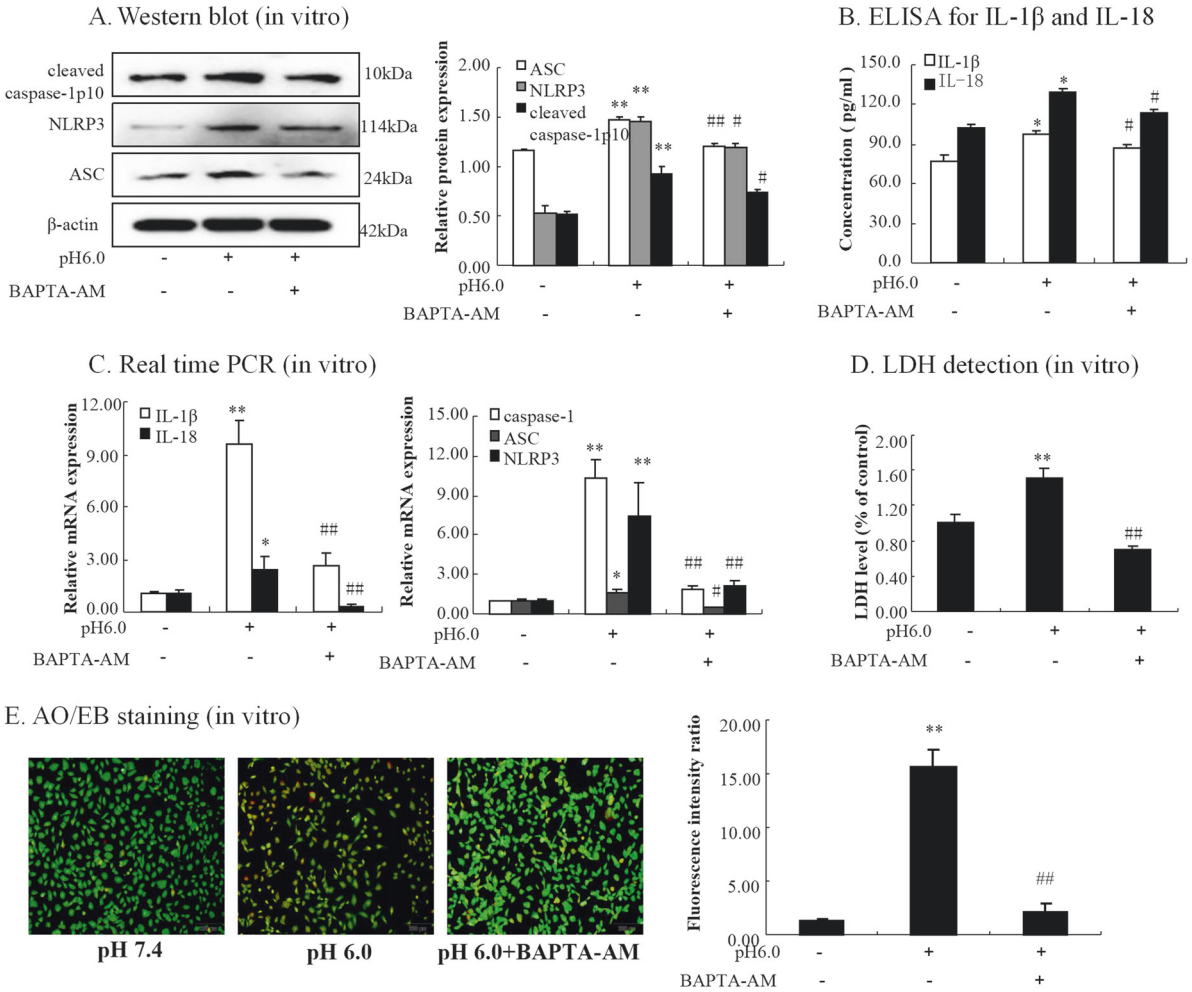

Fig. 7 Role of Ca^{2+} in extracellular acidosis-induced pyroptosis in primary articular chondrocytes. **a** Chelating agents of Ca^{2+} BAPTA-AM inhibited pyroptosis induced by extracellular acidosis in primary articular chondrocytes by western blotting for ASC, NLRP3 and cleaved caspase-1p10. **b** BAPTA-AM inhibited the levels of IL-1β and IL-18 in culture medium. **c** Effects of BAPTA-AM on extracellular acidosis-induced pyroptosis in primary articular chondrocytes by real-time PCR. **d** BAPTA-AM resisted the release of LDH in primary articular chondrocytes. **e** BAPTA-AM inhibited pyroptosis induced by extracellular acidosis in primary articular chondrocytes by AO/EB staining, semi-quantitative results. **f** BAPTA-AM reduced the levels of ASC and NLRP3 in primary articular chondrocytes by immunofluorescence. The data are presented as the mean ± SEM of three wells in three independent experiments, $^{*}P < 0.05$, $^{**}P < 0.01$ vs. pH 7.4 group; $^{\#}P < 0.05$, $^{\#\#}P < 0.01$ vs. pH 6.0 group

Acknowledgements We are particularly grateful to our colleagues and Feihu Chen.

Funding This project was supported by grants from the National Natural Science Foundation of China (Nos. 81271949 and 30873080).

Compliance with ethical standards

Conflict of interest The authors declare that they have no conflict of interest.

References

1. Branimir A, Miroslav M. Pathogenesis of rheumatoid arthritis. Reumatizam. 2014;6:19–23.
2. Crowson CS, Liao KP, Davis JM, et al. Rheumatoid arthritis and cardiovascular disease. Am Heart J. 2013;166:622–8e621.
3. Firestein GS. Evolving concepts of rheumatoid arthritis. Nature. 2003;423:356–61.
4. Foster MH. Basement membranes and autoimmune diseases. Matrix Biol. 2017;57–58:149–68.
5. Razaq S, Wilkins RJ, Urban JP. The effect of extracellular pH on matrix turnover by cells of the bovine nucleus pulposus. Eur Spine J. 2003;12:341–9.
6. Ahn H, Kim JM, Lee K, et al. Extracellular acidosis accelerates bone resorption by enhancing osteoclast survival, adhesion, and migration. Biochem Biophys Res Comm. 2012;418:144–8.
7. Astry B, Harberts E, Moudgil KD. A cytokine-centric view of the pathogenesis and treatment of autoimmune arthritis. J Interferon Cytokine Res. 2011;31:927–40.
8. Singh JA, Christensen R, Wells GA, et al. A network meta-analysis of randomized controlled trials of biologics for rheumatoid arthritis: a Cochrane overview. CMAJ. 2009;181:787–96.
9. Bianchi G, Caporali R, Todoerti M, et al. Methotrexate and rheumatoid arthritis: current evidence regarding subcutaneous versus oral routes of administration. Adv Ther. 2016;33:369–78.
10. Zampeli E, Vlachoyiannopoulos PG, Tzioufas AG. Treatment of rheumatoid arthritis: unraveling the conundrum. J Autoimmun. 2015;65:1–18.
11. Donahue KE, Gartlehner G, Jonas DE, et al. Systematic review: comparative effectiveness and harms of disease-modifying medications for rheumatoid arthritis. Ann Intern Med. 2008;148:124–34.
12. Leombruno JP, Einarson TR, Keystone EC. The safety of anti-tumour necrosis factor treatments in rheumatoid arthritis: meta and exposure-adjusted pooled analyses of serious adverse events. Ann Rheum Dis. 2009;68:1136–45.
13. Turesson C, Jacobsson LT, Matteson EL. Cardiovascular comorbidity in rheumatic diseases. Vasc Health Risk Manag. 2008;4:605–14.
14. Cookson BT, Brennan MA. Pro-inflammatory programmed cell death. Trends Microbiol. 2001;9:113–4.
15. Lamkanfi M, Dixit VM. Mechanisms and functions of inflammasomes. Cell. 2014;157:1013–22.
16. Lim Y, Kumar S. A single cut to pyroptosis. Oncotarget. 2015;6:36926–7.
17. De Nardo D, De Nardo CM, Latz E. New insights into mechanisms controlling the NLRP3 inflammasome and its role in lung disease. Am J Pathol. 2014;184:42–54.
18. Miao EA, Leaf IA, Treuting PM, et al. Caspase-1-induced pyroptosis is an innate immune effector mechanism against intracellular bacteria. Nat Immunol. 2010;11:1136–42.
19. von Moltke J, Ayres JS, Kofoed EM, et al. Recognition of bacteria by inflammasomes. Annu Rev Immunol. 2013;31:73–106.
20. Gross O, Thomas CJ, Guarda G, et al. The inflammasome: an integrated view. Immunol Rev. 2011;243:136–51.
21. Guarda G, So A. Regulation of inflammasome activity. Immunology. 2010;130:329–36.
22. Kang TB, Yang SH, Toth B, et al. Activation of the NLRP3 inflammasome by proteins that signal for necroptosis. Methods Enzymol. 2014;545:67–81.
23. Chavarria-Smith J, Mitchell PS, Ho AM, et al. Functional and evolutionary analyses identify proteolysis as a general mechanism for NLRP1 inflammasome activation. PLoS Pathog. 2016;12:e1006052.
24. de Torre-Minguela C, Mesa Del Castillo P, Pelegrin P. The NLRP3 and pyrin inflammasomes: implications in the pathophysiology of autoinflammatory diseases. Front Immunol. 2017;8:43.
25. Janowski AM, Colegio OR, Hornick EE, et al. NLRC4 suppresses melanoma tumor progression independently of inflammasome activation. J Clin Invest. 2016;126:3917–28.
26. Hu B, Jin C, Li HB, et al. The DNA-sensing AIM2 inflammasome controls radiation-induced cell death and tissue injury. Science. 2016;354:765–8.
27. Tschopp J, Martinon F, Burns K. NALPs: a novel protein family involved in inflammation. Nat Rev Mol Cell Biol. 2003;4:95–104.
28. Eldridge MJ, Shenoy AR. Antimicrobial inflammasomes: unified signalling against diverse bacterial pathogens. Curr Opin Microbiol. 2015;23:32–41.
29. Levy M, Thaiss CA, Katz MN, et al. Inflammasomes and the microbiota—partners in the preservation of mucosal homeostasis. Semin Immunopathol. 2015;37:39–46.
30. Dostert C, Petrilli V, Van Bruggen R, et al. Innate immune activation through Nalp3 inflammasome sensing of asbestos and silica. Science. 2008;320:674–7.
31. Suzuki H, Sozen T, Hasegawa Y, et al. Caspase-1 inhibitor prevents neurogenic pulmonary edema after subarachnoid hemorrhage in mice. Stroke. 2009;40:3872–5.
32. Duewell P, Kono H, Rayner KJ, et al. NLRP3 inflammasomes are required for atherogenesis and activated by cholesterol crystals. Nature. 2010;464:1357–61.
33. Kastbom A, Verma D, Eriksson P, et al. Genetic variation in proteins of the cryopyrin inflammasome influences susceptibility and severity of rheumatoid arthritis (the Swedish TIRA project). Rheumatology. 2008;47:415–7.
34. Choulaki C, Papadaki G, Repa A, et al. Enhanced activity of NLRP3 inflammasome in peripheral blood cells of patients with active rheumatoid arthritis. Arthritis Res Ther. 2015;17:257.
35. Vande Walle L, Van Opdenbosch N, Jacques P, et al. Negative regulation of the NLRP3 inflammasome by A20 protects against arthritis. Nature. 2014;512:69–73.
36. Rajamaki K, Nordstrom T, Nurmi K, et al. Extracellular acidosis is a novel danger signal alerting innate immunity via the NLRP3 inflammasome. J Biol Chem. 2013;288:13410–9.
37. Oorni K, Rajamaki K, Nguyen SD, et al. Acidification of the intimal fluid: the perfect storm for atherogenesis. J Lipid Res. 2015;56:203–14.
38. Gonzalez-Inchauspe C, Urbano FJ, Di Guilmi MN, et al. Acid-sensing ion channels activated by evoked released protons modulate synaptic transmission at the mouse calyx of held synapse. J Neurosci. 2017;37:2589–99.
39. Yuan FL, Chen FH, Lu WG, et al. Acid-sensing ion channel 1a mediates acid-induced increases in intracellular calcium in rat articular chondrocytes. Mol Cell Biochem. 2010;340:153–9.
40. Hu W, Chen FH, Yuan FL, et al. Blockade of acid-sensing ion channels protects articular chondrocytes from acid-induced apoptotic injury. Inflamm Res. 2012;61:327–35.

41. Rong C, Chen FH, Jiang S, et al. Inhibition of acid-sensing ion channels by amiloride protects rat articular chondrocytes from acid-induced apoptosis via a mitochondrial-mediated pathway. Cell Biol Int. 2012;36:635–41.
42. Bhowmick S, Moore JT, Kirschner DL, et al. Acidotoxicity via ASIC1a mediates cell death during oxygen glucose deprivation and abolishes excitotoxicity. ACS Chem Neurosci. 2017;8:1204–12.
43. Waldmann R, Champigny G, Bassilana F, et al. A proton-gated cation channel involved in acid-sensing. Nature. 1997;386:173–7.
44. Yermolaieva O, Leonard AS, Schnizler MK, et al. Extracellular acidosis increases neuronal cell calcium by activating acid-sensing ion channel 1a. Proc Natl Acad Sci USA. 2004;101:6752–7.
45. Yao H, Haddad GG. Calcium and pH homeostasis in neurons during hypoxia and ischemia. Cell Calcium. 2004;36:247–55.
46. Barton A, Worthington J. Genetic susceptibility to rheumatoid arthritis: an emerging picture. Arthritis Rheum. 2009;61:1441–6.
47. Carlens C, Hergens MP, Grunewald J, et al. Smoking, use of moist snuff, and risk of chronic inflammatory diseases. Am J Resp Crit Care Med. 2010;181:1217–22.
48. Lee AS, Ellman MB, Yan D, et al. A current review of molecular mechanisms regarding osteoarthritis and pain. Gene. 2013;527:440–7.
49. Duncan JA, Bergstralh DT, Wang Y, et al. Cryopyrin/NALP3 binds ATP/dATP, is an ATPase, and requires ATP binding to mediate inflammatory signaling. Proc Natl Acad Sci USA. 2007;104:8041–6.
50. Kolly L, Busso N, Palmer G, et al. Expression and function of the NALP3 inflammasome in rheumatoid synovium. Immunology. 2010;129:178–85.
51. Choi AJ, Ryter SW. Inflammasomes: molecular regulation and implications for metabolic and cognitive diseases. Mol Cells. 2014;37:441–8.
52. Sui J, Li H, Fang Y, et al. NLRP1 gene polymorphism influences gene transcription and is a risk factor for rheumatoid arthritis in han chinese. Arth Rheum. 2012;64:647–54.
53. Segovia J, Sabbah A, Mgbemena V, et al. TLR2/MyD88/NF-kappaB pathway, reactive oxygen species, potassium efflux activates NLRP3/ASC inflammasome during respiratory syncytial virus infection. PLoS ONE. 2012;7:e29695.
54. Franchi L, Warner N, Viani K, et al. Function of Nod-like receptors in microbial recognition and host defense. Immunol Rev. 2009;227:106–28.